Pseudogenization of the *cntQ* permease confers distinct yersinopine-metal uptake selectivity in *Yersinia* species

Running title: Role of yersinopine and permease CntQ in Yersinia

Clémentine Laffont[a,*], Elizabeth Pradel[b], Laurent Ouerdane[c], Amélie Brodel[b], Nicolas Oswaldo Gomez[d,§], Anaïs Hujeux[b], Mathilde Tribout[a,¶], Catherine Brutesco[a], Romé Voulhoux[d], Ryszard Lobinski[c], Florent Sebbane[b], Pascal Arnoux[a]

[a]Aix-Marseille University, French Alternative Energies and Atomic Energy Commission (CEA), French National Center for Scientific Research (CNRS), UMR7265 Institute of Biosciences and Biotechnologies of Aix-Marseille (BIAM), Saint-Paul-lez-Durance, 13108, France.

[b]Univ. Lille, Inserm, CNRS, CHU Lille, Institut Pasteur Lille, U1019-UMR 9017-CIIL-Center for Infection and Immunity of Lille, F-59000 Lille, France.

[c]Universite de Pau et des Pays de l'Adour, e2s UPPA, CNRS, IPREM-UMR5254, Hélioparc, Pau, France.

[d]Laboratoire de Chimie Bactérienne (LCB) UMR7283, Institut de Microbiologie de la Méditerranée (IMM), CNRS, Aix-Marseille Université, Marseille, France.

[*]Present address: Department of Quantitative Biomedicine, University of Zurich, Winterthurerstrasse 190, 8057 Zürich, Switzerland.

¶ Present address: [d]Laboratoire de Chimie Bactérienne (LCB) UMR7283, Institut de Microbiologie de la Méditerranée (IMM), CNRS, Aix-Marseille Université, Marseille, France.

[§]Present address: Department of Molecular Bacteriology, Helmholtz Centre for Infection Research, 38124 Braunschweig, Germany.

Correspondence: florent.sebbane@inserm.fr; pascal.arnoux@cea.fr

Abstract

Yersinopine is a nicotianamine-like metallophore recently inferred from a biochemical study, however its production *in vivo* and functional role have not been evaluated. Intriguingly, the *Yersinia pestis cnt* operon (*cntPQRLMI*) encoding yersinopine biosynthesis and transport (with *cntPQR* encoding a predicted ABC transport system, *cntLM* the two biosynthetic enzymes and *cntI* the predicted yersinopine exporter) shows two frameshift mutations in the *cntQ* gene encoding the permease, whereas this gene appears intact in *Yersinia pseudotuberculosis*. This pseudogenization, which occurred during the emergence of *Y. pestis* from *Y. pseudotuberculosis,* questions the role of yersinopine (if any) in both species. Here we show that yersinopine is secreted by both *Y. pestis* and *Y. pseudotuberculosis* in metal scarce conditions, and expression of the operon is repressed by the zinc uptake regulator (Zur). Surprisingly, the *cnt* operon was found to be involved in iron uptake in *Y. pseudotuberculosis* whereas it played a role in zinc acquisition in *Y. pestis*. Furthermore, mutation of *cntQ* in *Y. pseudotuberculosis* triggered a switch from iron import to zinc import, therefore recapitulating the phenotype observed in *Y. pestis*. This work demonstrates the production of yersinopine in two closely related bacteria in zinc scarce conditions, and highlights the effect of a pseudogenization event triggering a global change in metal uptake specificity.

IMPORTANCE *Yersinia pestis*, the bacteria responsible for plague, emerged from *Yersinia pseudotuberculosis* less than 6.000 years ago. Genetically close, only a few acquisition and loss of genes played a crucial role in the emergence of flea-borne plague. In this context, the *cnt* operon encoding the yersinopine metallophore biosynthesis, export and recovery of the metal-yersinopine complexes appears complete in *Y. pseudotuberculosis.* In contrast, a frameshift mutation impairs the permease CntQ in *Y. pestis*. This questions whether these species can produce and use yersinopine and, if so, what would be the impact on their metal uptake. Here, we report the production of the metallophore yersinopine in both bacteria, though it is used for iron uptake in *Y. pseudotuberculosis* whereas it is important for zinc uptake in *Y. pestis*. By introducing a frameshift mutation in the *cntQ* gene of *Y. pseudotuberculosis*, we observed a shift toward zinc uptake, recapitulating an event that happened during the emergence of *Y. pestis* from its ancestor.

Introduction

Metal uptake is a cornerstone process for all living organisms, as the metals serve as catalytic and/or structural co-factors for proteins involved in essential metabolic reactions. Bacteria encode in their genomes an array of machineries to ensure metal uptake, depending on the availability of these resources in the biotopes they inhabit (1, 2). Generally, when in abundance or bioavailable, metals are directly acquired from the environment through metal uptake systems (such as ABC transporters) able to import the free metallic form. However, when facing metal scarce conditions, bacteria use high affinity acquisition pathways, relying either on the acquisition of metal containing molecules (such as haem) or the production, secretion, and uptake of metallophores like siderophores that are specialized in iron uptake. Altogether, these high affinity pathways endow bacteria the capacity to access resources otherwise unreachable. These machineries are particularly useful for pathogenic bacteria that have to face the nutritional immunity of their host (3–6). Indeed, while the immune system of the host tries to limit bacterial growth by sequestering metals or by bombarding the bacteria with toxic doses, bacteria have evolved efficient mechanisms to maintain metal homeostasis. Among these systems, nicotianamine-like metallophores such as staphylopine and pseudopaline have been described as involved in the acquisition of various metals in *Staphylococcus aureus* and *Pseudomonas aeruginosa* respectively (7, 8). There is however increasing evidence these metallophores are involved in the acquisition of zinc in a chelating environment produced by the host (8–10), though some experiments show that they might be involved in the import of iron or nickel (7, 8, 11) , or even play a role in copper intoxication (12). Additionally, the *cnt* operon controlling staphylopine production, secretion and staphylopine-metal recovery is under the control of both zinc and iron levels in *S. aureus* (13). Mostly studied in these two opportunistic human pathogens, bacterial nicotianamine-like metallophores are much more widespread, both among pathogenic or environmental bacteria (11, 14). Recently, a biochemical study inferred the existence of a novel nicotianamine-like metallophore called yersinopine by studying the opine dehydrogenase CntM activity from *Y. pestis* (15), although its production and role *in vivo* have not been demonstrated.

Y. pestis causes plague, a fatal disease mainly transmitted by fleas. It recently emerged from *Y. pseudotuberculosis*, an enteropathogen causing benign enteric infection following the ingestion of contaminated food in humans (16). We still have a partial view of the mechanisms

that led to the emergence of *Y. pestis* from *Y. pseudotuberculosis*. However, we know that acquisition and loss of a few genes played a crucial role in the emergence of flea-borne plague with high incidence (17, 18). For instance, a frameshift mutation in the *ureD* gene, which abolished the nickel-dependent urease of *Y. pestis,* was a key step to increase the incidence of flea-borne plague because it drastically decreased the toxicity of *Y. pseudotuberculosis* towards fleas (19, 20). In this context, it is interesting to note that *Y. pseudotuberculosis* possesses a predicted functional *cntPQRLMI* operon [with genes predicted to govern the synthesis (*cntLM*) and export (*cntI*) of yersinopine, and the recovery of yersinopine-metal complexes through an ABC transporter (cntPQR)], while the *cntQ* gene of *Y. pestis* seems non-functional due to two frameshift mutations (Figure 1). This pattern of a full *cntQ* permease gene in *Y. pseudotuberculosis* and a pseudogenization of this gene in *Y. pestis* is conserved in many different strains (Supplementary Table 1). Considering that only *cntQ* is mutated in *Y. pestis*, one may wonder whether yersinopine is synthesized and secreted by this bacterium and, if so, whether or not it plays a role in metal uptake in *Y. pestis* and *Y. pseudotuberculosis*. Yersinopine is a staphylopine epimer, and staphylopine has been linked to urease activity in *Staphyloccocus aureus* (21), suggesting that there might also be a link between a mutation on *cntQ* and the loss of urease activity in *Y. pestis*. Overall, although this frameshift mutation in the ABC transporter permease *cntQ* (sometimes called *fiuA* or *fhuD*) was early recognized, its function was not studied in detail (22, 23). *Y. pestis* is well equipped for iron and zinc uptake to face the nutritional immunity of the host, *via* the production of numerous siderophores (23), the import of zinc through ZnuABC (24, 25) and also the production of yersiniabactin, a siderophore that is also involved in zinc uptake (26, 27). The presence of a *cnt* operon in *Y. pseudotuberculosis* and the detection of a frameshift mutation in the gene encoding the permease in *Y. pestis* therefore questions whether these species can produce and use yersinopine and, if so, what would be the metal transported through this system.

In order to address these questions, we confirmed the pathway of yersinopine biosynthesis *in vitro*, and verified its production and secretion *in vivo* by *Y. pestis* and *Y. pseudotuberculosis* using the same chemically defined growth medium. We also investigated the regulation of both *cnt* operons and confirmed their regulation by the Zur repressor. By comparing WT and mutant strains devoid of the *cnt* operon in both species, we unexpectedly found that the Cnt system is responsible for iron uptake in *Y. pseudotuberculosis* whereas it is important for zinc uptake in *Y. pestis*. Finally, by introducing a frameshift mutation in the *cntQ* gene of *Y.*

pseudotuberculosis, we observed a shift toward zinc uptake, establishing that such an evolutionary event could indeed lead to the evolution of metal uptake specificity.

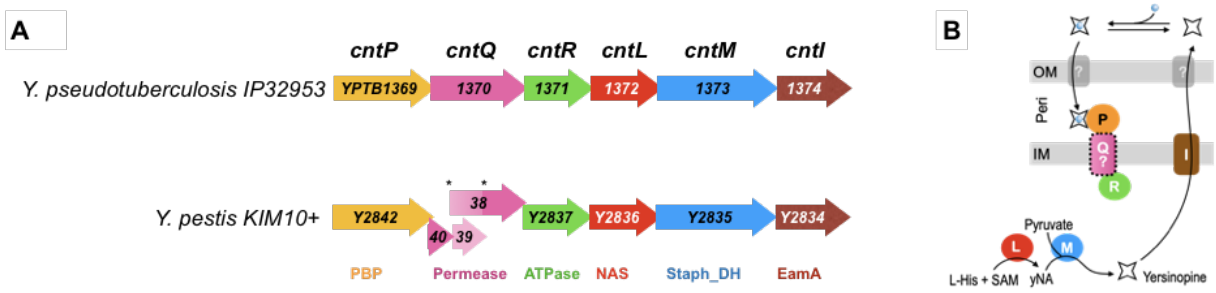

Figure 1: Comparison of the *cnt* operon structure in *Y. pseudotuberculosis* and *Y. pestis*. (A) Two single base deletions in the *Y. pestis* genomes as compared to *Y. pseudotuberculosis* are marked with stars. The first deletion causes a frameshift mutation in the *cntQ* gene of *Y. pestis* and leads to a premature stop codon in the first ORF (Y2840, 83 amino acids). The next putative ORF (Y2839, 130 amino acids) is frameshifted as compared to the *cntQ* ORF from *Y. pseudotuberculosis*. The beginning of the third ORF (Y2838; corresponding to residue 1-117) is also frameshifted, although the second deletion leads to a recovery of the same reading frame as the *Y. pseudotuberculosis cntQ* gene for the last 162 residues (amino acids 118 to 280 are identical to YPTB1370 residues 190 to 352). These three *Y. pestis* predicted ORFs, alone or together, are very unlikely to lead to a functional permease. The frameshifted regions as compared to *Y. pseudotuberculosis* ORFs are indicated with a light color. The other proteins encoded by the operons share between 99.3% (CntL) and 100% sequence identity (CntM and CntI). (B) Model of yersinopine biosynthesis, export and recovery of metal-yersinopine complexes in the periplasm of *Yersinia* species. In this context, what would be the role (if any) of an ABC transporter with a defective CntQ permease, such as found in *Y. pestis*?

Biochemical evidence that yersinopine is produced by *Y. pseudotuberculosis*

Yersinopine production was previously inferred through biochemical assays examining the activity of the CntM enzyme from *Y. pestis* by steady state kinetic (15). However, the entire biosynthetic pathway was not explored in that study. Here, we completed the pathway by studying the activity of the purified recombinant enzymes YpCntL and YpCntM from *Y. pseudotuberculosis* using different biochemical assays. First, we investigated the activity of YpCntL and YpCntM using a ^{14}C-labelled SAM substrate assay. In this assay, the aminobutyrate moiety of SAM is followed thanks to the ^{14}C labelling and subsequent separation on a TLC plate. Using the ^{14}C-labelled SAM substrate assay we showed that YpCntL was specific to L-

histidine (Figure 2A) and, by co-incubation with other substrates, we confirmed that YpCntM used NADPH to reductively condensate the yNA pathway intermediate with pyruvate to produce yersinopine (Figure 2B). This was further verified by HILIC/ESI-MS separation and detection, which validated the use of L-Histidine (Figure 2C) and pyruvate (Figure 2D) respectively by YpCntL and YpCntM leading to yersinopine production. Overall, we demonstrated that CntL and CntM from *Y. pseudotuberculosis* catalyze the formation of yersinopine according to the reaction pathway shown in Figure 2E. Given the high sequence identity of CntL (99.3%) and CntM (100%) between *Y. pseudotuberculosis* and *Y. pestis*, we conclude that if *Y. pestis* produces a metallophore, it is likely identical to that of *Y. pseudotuberculosis*, specifically yersinopine.

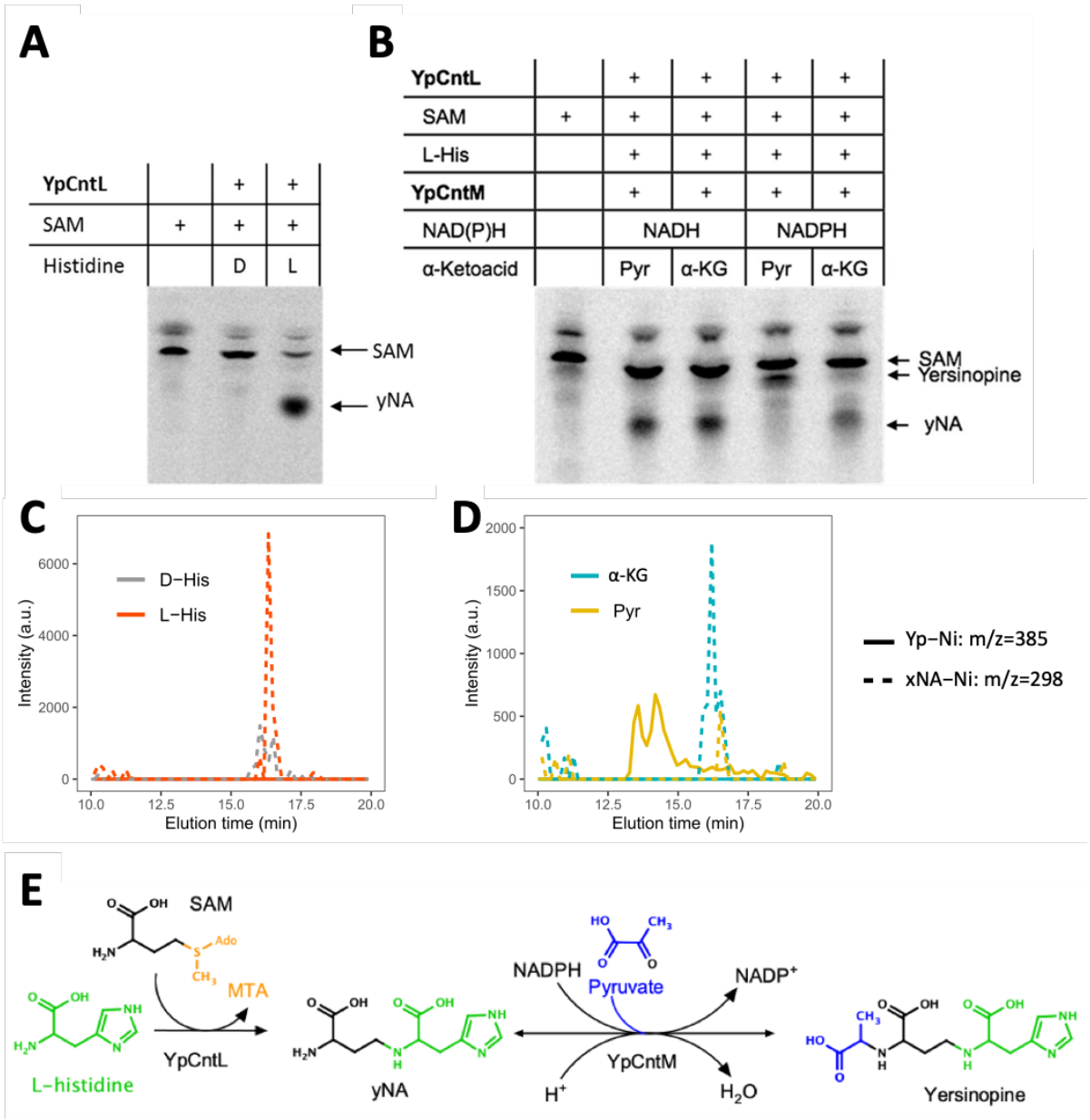

Figure 2: *In vitro* selectivity of YpCntL and YpCntM. (A-B) Radiograms of a TLC plate after migration of samples corresponding to the incubation of YpCntL with ^{14}C-SAM and L- or D-Histidine (A) and the co-incubation of YpCntL with its substrates (L-Histidine and ^{14}C-SAM) and YpCntM with possible substrates (Pyruvate or α-ketoglutarate (α-KG)) and cofactors (NAD(P)H) (B). (C-D) HILIC/ESI-MS separation and detection of the pathway intermediate xNA and yersinopine in complex with nickel after incubation of YpCntL with SAM and L- or D-Histidine (C) and after the co-incubation of YpCntL with its substrates (L-Histidine and SAM) and YpCntM with possible substrates (Pyruvate or α-KG) and its cofactor NADPH. (E) Overall yersinopine biosynthetic pathway.

Yersinopine is produced and exported by both *Y. pseudotuberculosis* and *Y. pestis*

Knowing the role of CntL and CntM in yersinopine biosynthesis and inferring the role of CntI in yersinopine export across the inner membrane (8, 15, 28), we aimed to determine whether yersinopine is synthesized and exported by both *Y. pestis* and *Y. pseudotuberculosis*. To investigate this, yersinopine was measured by HILIC/ESI-MS in the extracellular fractions of *Y. pseudotuberculosis* and *Y. pestis* grown in the minimal medium TMH (Figure 3). The culture supernatants were analyzed by separating them on a HILIC column coupled with ESI-MS analyses to identify precise masses. Yersinopine was found complexed with multiple divalent metals, predominantly zinc, and to a lesser extent copper, nickel, and cobalt. This reflects the higher affinity of zinc for this metallophore under these experimental conditions. Iron(II)-yersinopine complexes were not detected due to technical limitations, specifically oxidation under aerobic conditions. Notably, divalent metal-yersinopine complexes were identified in both species, although the overall intensity of the HILIC/ESI-MS signal was lower for *Y. pestis*, which indicates a reduced concentration of extracellular yersinopine in *Y. pestis* compared to *Y. pseudotuberculosis*. Overall, the detection of yersinopine in the extracellular fractions of both species not only confirms that both *Y. pestis* and *Y. pseudotuberculosis* produce and export this metallophore, but also that the pseudogenization of the CntQ permease in *Y. pestis* does not impair the function of upstream operon genes, allowing for the production and export of yersinopine.

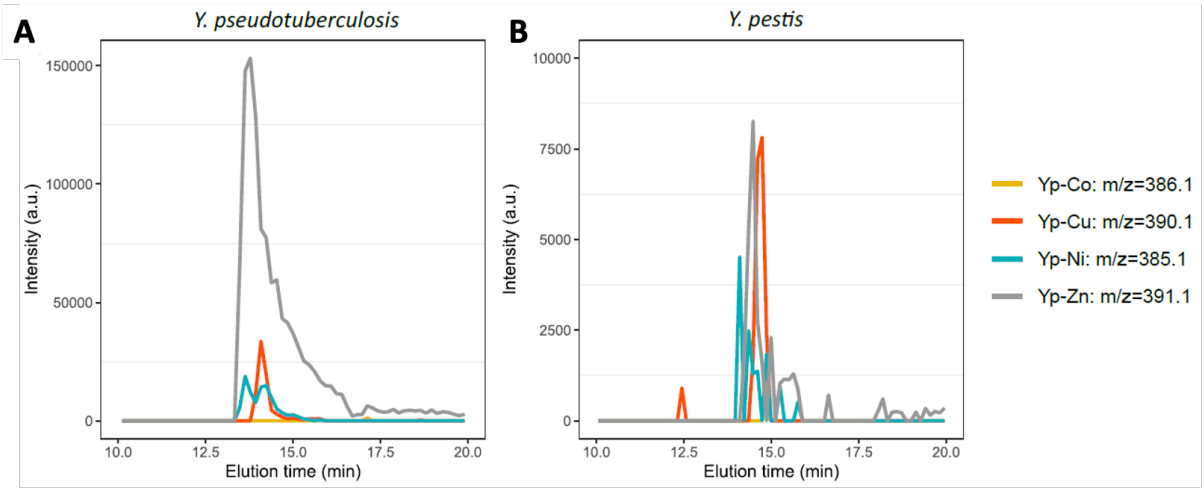

Figure 3: *In vivo* production and secretion of yersinopine by *Y. pseudotuberculosis* and *Y. pestis*. HILIC/ESI-MS separation and detection of various divalent metal-yersinopine complexes in the culture supernatants of *Y. pseudotuberculosis* (A) and *Y. pestis* (B).

The *cnt* operon is repressed by Zur in both *Y. pseudotuberculosis* and *Y. pestis*

Having established the production and secretion of yersinopine in *Y. pseudotuberculosis* and *Y. pestis,* we sought to confirm the involvement of the Zur repressor in the regulation of the *cnt* operon. The Zur regulon was previously investigated in *Y. pestis* microtus (24, 29) and in *Y. pseudotuberculosis* (30). In the absence of Zur, *cntP* was the most up-regulated gene (227 fold-change in *Y. pestis*, 9 fold change in *Y. pseudotuberculosis*) and, overall, the downstream genes in the operon were also upregulated (from 45 fold-change for *cntQ* to 6 for *cntI* in *Y. pestis*, and 5-6 fold for *cntQR* in *Y. pseudotuberculosis*). However, at the time of these studies, the function of the *cnt* system was unknown and it was not further characterized. In *Y. pseudotuberculosis,* the Zur regulon was also investigated through the role of the Znu zinc uptake system, suggesting a role of zinc in the defence against reactive oxygen stresses (31). To confirm the involvement of the Zur repressor in the regulation of the *cnt* operon in both *Y. pestis* and *Y. pseudotuberculosis,* we introduced a *lacZ* reporter fusion downstream of the *cnt* promoter into the chromosome of Zur+ and Zur- strains for each species. As expected, in a rich medium, the *cnt* promoter was repressed in the Zur+ strains whereas it is not in the mutants lacking Zur (Figure 4), which validates the involvement of Zur in the regulation of the *cnt* operon in both species.

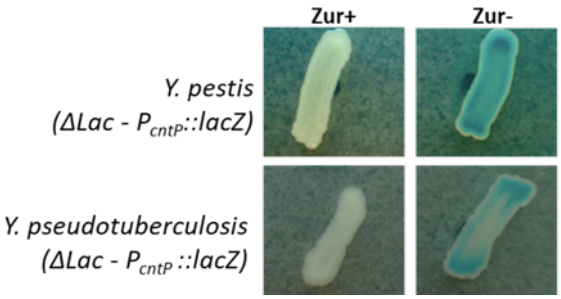

Figure 4: Expression of the *cnt* operon in *Y. pestis* and *Y. pseudotuberculosis* Δlac Zur+/Zur- pairs. Each strain was deleted from the β-galactosidase gene and carried a chromosomal fusion between the *cnt* operon promoter (*cntPp*) and the *E. coli lacZ* reporter gene. β-galactosidase activity was detected by the development of a blue color after growth on LB-agar plates supplemented with X-gal.

Yersinopine mediates distinctive strategies of metal uptake in *Y. pseudotuberculosis* and *Y. pestis*

After showing that the *cnt* operon is repressed by Zur and is involved in the production and secretion of yersinopine in both *Y. pseudotuberculosis* and *Y. pestis*, we examined the impact

of gene deletions in the Cnt system on metal accumulation. We constructed several deletion strains in both species, either deleting *cntQ* with a polar effect on downstream genes making it unable to produce yersinopine (noted Δ*cntQ(RLMI)*) or deleting *cntLMI* (noted Δ*cntLMI*; see method for mutant generation and strains description). Additionally, in *Y. pseudotuberculosis* we deleted the *cntQ* gene (noted Δ*cntQ*) without polar effect, so this loss would ideally phenocopy the *cnt* operon of *Y. pestis*. We first observed that, when supplementing the TMH culture medium with increasing concentration of EDTA (a metal chelator frequently used to induce metal starvation), the growth rate of *Y. pseudotuberculosis* wild-type strain increased whereas that of the different *cnt* deletion strains decreased (Supplementary Figure S1). This suggests that the *cnt* operon provides a growth advantage in an EDTA metal-chelated environment, and eventually suggests that EDTA-metal complexes might be used as a source of essential metal. Therefore, in order to compare *Y. pseudotuberculosis* with *Y. pestis*, and mutants within each species, we decided to compare metal accumulation using TMH medium without EDTA supplementation, as we had also identified yersinopine production in this medium for both *Y. pseudotuberculosis* and *Y. pestis*. Intracellular metal content of wild-type and mutant strains were estimated by ICP-MS. Surprisingly, in *Y. pseudotuberculosis* we found that the absence of yersinopine biosynthetic genes (in both Δ*cntQ(RLMI)* and Δ*cntLMI* strains) slightly but significantly reduced iron content (-27.6%; $p=3.7.10^{-5}$ and -31.1%; $p=4.5.10^{-3}$ respectively), but had no effect on zinc or other metal uptake (Figure 5A). This decrease of intracellular iron was restored to the wild-type level in a complemented strain, overall suggesting that the Cnt system is an iron uptake system in *Y. pseudotuberculosis*. The mutant lacking only the *cntQ* gene will be described after the comparison of wild-type and mutant strains of *Y. pestis* detailed in the next paragraph, as it mimics the situation found in *Y. pestis*. In *Y. pestis,* the iron content was similar in the wild-type and *cnt* mutant strains, whereas we observed a significant decrease in intracellular zinc in both Δ*cntQ(RLMI)* and Δ*cntLMI* mutants (by 47.3%, $p=6.2.10^{-3}$ and by 50.9% $p=1.9.10^{-2}$ respectively; Figure 5B). This suggests that the *cnt* operon is involved in zinc uptake in *Y. pestis*, which was somehow unexpected as *cntQ* is a pseudogene in this species. Another trend observed in *Y. pestis* was an important increase in cobalt content in the *cnt* mutants (Δ*cntQ(RLMI*) or Δ*cntLMI*) as compared to the wild-type (by 176.4%, $p=2.8\ 10^{-6}$ and by 182.2%, not significant due to high variation in replicates respectively).

To determine whether there was any additional effect of zinc transporters on zinc uptake and a cross-talk between cobalt uptake and yersinopine production, we measured zinc and cobalt levels in *Y. pestis Δcnt* mutants, additionally lacking either the yersiniabactin importer YbtX (which mediates yersiniabactin-zinc uptake), or the Znu system (which mediates free zinc uptake), or lacking both YbtX and Znu systems (Figure 5C). Compared to the yersinopine deficient mutant, we did not observe a further decrease in intracellular zinc concentration in the double and triple mutants, which suggests that unknown zinc uptake mechanisms are still at work. In contrast, we observed a wild-type level of intracellular cobalt in the two Δ*cnt* mutants also lacking the Znu system (Δ*cnt* Δ*znu* and Δ*cnt* Δ*ybtX* Δ*znu)*, whereas cobalt level remained high in the mutant lacking either Cnt or both Cnt and YbtX. This suggests that, in the absence of yersinopine, cobalt could be efficiently imported through the Znu transporter. Conversely, the presence of yersinopine could prevent cobalt uptake through the Znu system in *Y. pestis*.

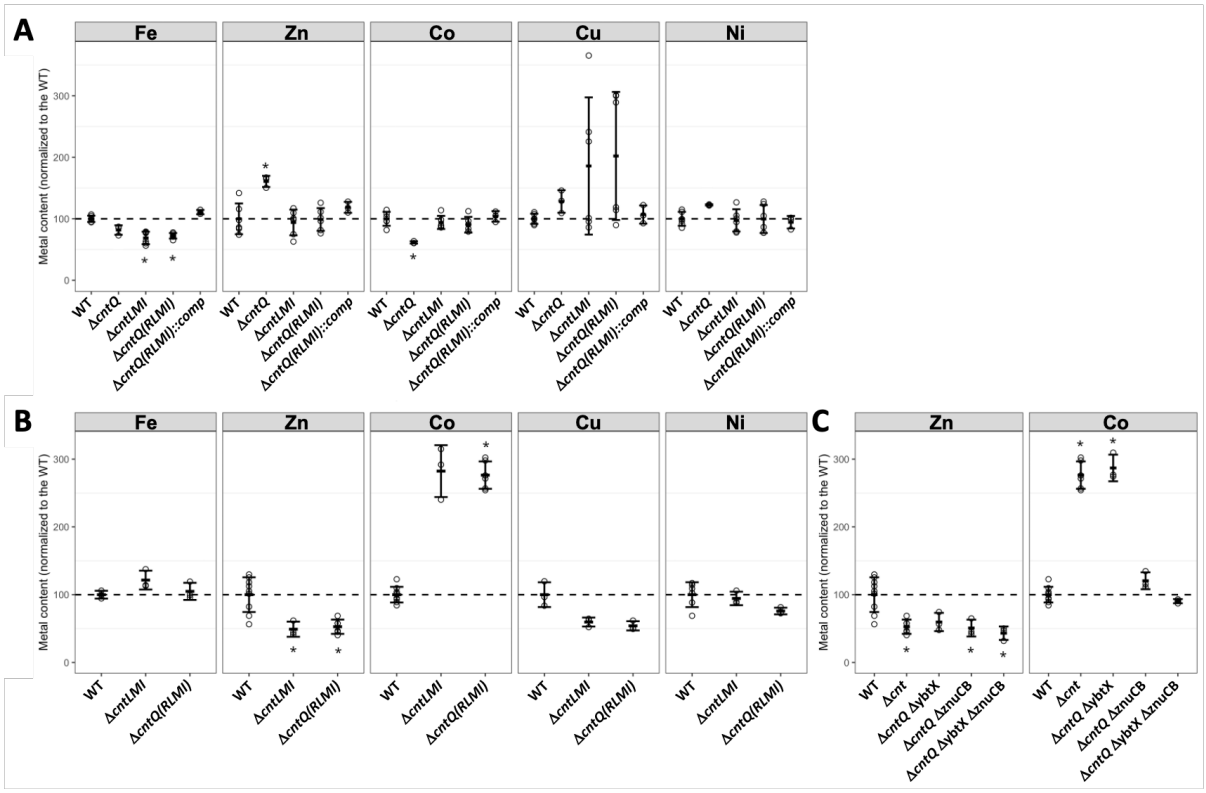

Figure 5: ICP-MS measurement of intracellular metal levels in *Y. pseudotuberculosis* and *Y. pestis* wild-type and deletion strains. (A) Intracellular metal levels in *Y. pseudotuberculosis* wild-type (WT) and deletion strains. (B) Intracellular metal levels in *Y. pestis* WT and deletion strains. (C) Intracellular zinc and cobalt levels in *Y. pestis* WT and deletion strains lacking the Cnt system in combination with the yersiniabactin and

Znu systems. *indicates a p-value < 0.05 when comparing the metal content in the mutant versus the WT strain (welch test with Bonferroni correction).

Deletion of *cntQ* in *Y. pseudotuberculosis* recapitulates the evolution of metal-uptake specificity

Our above data suggest that the pseudogenization of the *cntQ* permease gene in *Y. pestis* changed metal-uptake specificity during its emergence from *Y. pseudotuberculosis*. To test this hypothesis, we studied the impact of the loss of *cntQ* on *Y. pseudotuberculosis* metal uptake, which mimics the situation found in *Y. pestis*. We found that the decrease in the intracellular level of iron observed in the strains unable to produce yersinopine (Δ*cntQ(RLMI*) or Δ*cntLMI*) compared to the wild-type was no longer detectable. However, the deletion of *cntQ* triggered an increase in the intracellular level of zinc and a decrease in that of cobalt (by 60.8%, $p=2.5.10^{-2}$ and by 38.4%, $p=5.8.10^{-3}$ respectively; Figure 5A). This phenocopies the *Y. pestis* wild-type phenotype as in this bacterium the Cnt system participates in zinc transport and prevents cobalt entry. Therefore, production of yersinopine combined with an incomplete yersinopine importer in the *cntQ* mutant of *Y. pseudotuberculosis* switched the overall transport towards zinc uptake, and likely prevented cobalt entry through the Znu transporter, similar to what occurs in *Y. pestis*.

Discussion

A functional pathway of yersinopine-mediated metal uptake system (*cntPQRLMI*) was predicted in *Y. pseudotuberculosis*, but the presence of a frameshift mutation in the *cntQ* permease gene suggested that this system was non-functional in *Y. pestis* (23). Pseudogenes are particularly abundant in the genome of *Y. pestis* as compared to *Y. pseudotuberculosis*, accounting for up to 8% of its genes, yet their functional impact remains to be studied for most of these events (32). Here we detected yersinopine in the extracellular fraction of both species using the same low-zinc growth medium, which indicates that yersinopine production and secretion are not impaired by the inactive *cntQ* gene of *Y. pestis*. This also aligns with transcriptomic data showing that the *Y. pestis cnt* operon is controlled by the Zur repressor (29), and is highly expressed during pneumonic infection (22). Together, these findings support the conclusion that the *cnt* operon remains functional. An important question is therefore the role of yersinopine in the context of either a complete Cnt system (as seen in *Y. pseudotuberculosis*) or a system lacking the permease of the ABC transporter (as in *Y. pestis*). Our data suggest that the Cnt system is not involved in nickel uptake in *Y. pestis* and *Y. pseudotuberculosis*, contrary to what was found in the case of *P. aeruginosa* (8, 9). This finding implies that this system is not associated with the nickel-dependent urease present in *Y. pseudotuberculosis*. Surprisingly, our data rather demonstrate that the presence/absence of the CntQ permease is linked to metal uptake specificity in *Yersinia*, from an iron uptake system when CntQ is present such as in *Y. pseudotuberculosis*, to a zinc uptake system when CntQ is absent such as in *Y. pestis*. To our knowledge, this is a unique observation of such a shift in substrate specificity upon pseudogenization of a permease associated with an ABC transporter. In *Y. pestis*, a frameshift mutation was found in the *iucA* gene involved in the aerobactin siderophore biosynthesis. However, the bacteria are still able to use aerobactin-iron complexes for iron uptake, presumably through piracy of aerobactin produced by other bacteria in the biotope and thanks to a functional uptake system (33).

The role of the Znu system in zinc uptake was extensively studied in *Y. pestis*. This system was not found to be essential for virulence, which indicates the presence of at least one additional zinc-uptake system (24). However, the authors dismissed a role of the periplasmic binding protein CntP (Y2842, originally called FiuA) in zinc uptake on the basis that a Δ*cntP* mutant grew like the wild-type, Δ*znuACB* or Δ*znuACB* Δ*cntP* strains in low zinc condition. Yet, by showing here the importance of the *cnt* operon for zinc uptake in *Y. pestis*, our work reveals a

further level of complexity. While the entire cnt operon seems crucial for zinc uptake, the specific role of CntP is still unclear. Indeed, we don't know yet if it is rerouted to another transporter, or if it exerts an indirect role, for example by chelating a yersinopine-metal complex. The fact that the CntQ permease is impaired in *Y. pestis* argues more in favor of a role of yersinopine through a *cntPQR*-independent route. In this context it would be interesting to study the mutant lacking *cntPQR* in both *Y. pestis* and *Y. pseudotuberculosis* to see whether CntP is directly involved in metal uptake.

The increased cobalt intracellular accumulation in *Y. pestis* upon inactivating the *cnt* operon was surprising. However, we also found that this increase was correlated with the presence of a functional Znu system, as the absence of both Cnt and Znu systems reduced intracellular cobalt accumulation back to the wild-type level. This interplay between the Znu and Cnt systems could be explained by the possibility of yersinopine to form a complex with cobalt in the periplasmic space, which would prevent its entry into the cytoplasm via the Znu system. A connection between Znu and cobalt has been described in *P. aeruginosa* (9, 34), where cobalt uptake was found to be increased in a mutant lacking the Znu ABC transporter, suggesting a zinc-regulated cobalt uptake mechanism. Though opposite, these works and the present study highlight that cross-talks between zinc and cobalt uptake systems are frequent. A model recapitulating zinc and cobalt import through the Cnt and Znu systems in both *Y. pseudotuberculosis* and *Y. pestis* is presented in Figure 6.

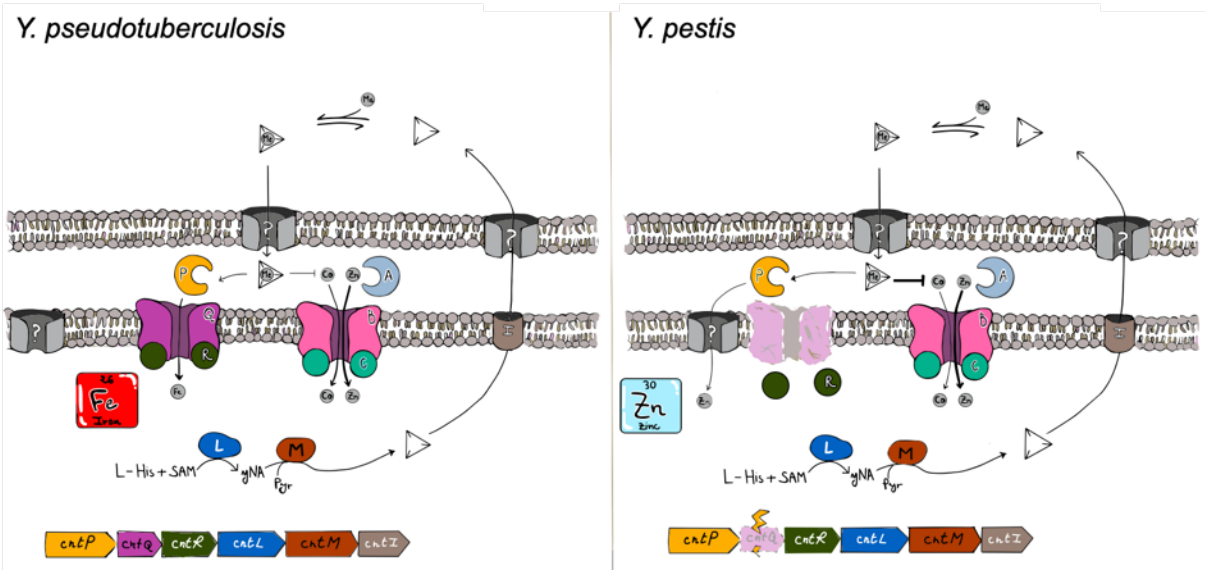

Figure 6: Comparative model of metal uptake through the Cnt and Znu systems in *Y. pseudotuberculosis* (left) and *Y. pestis* (right). In *Y. pseudotuberculosis*, yersinopine-metal complexes in the periplasm participate in iron uptake, presumably through the CntPQR ABC transporter encoded in the *cnt* operon. In *Y. pestis*, the absence of the CntQ permease, due to a frameshift mutation in its gene, leads to a different metal uptake specificity as compared to *Y. pseudotuberculosis*: the observed import of zinc through the Cnt system would occur by rerouting of the yersinopine-zinc complex toward an unknown uptake system (noted "?" in the inner membrane), either or not through an interaction with CntP in the periplasm. In both *Yersinia* species, in the outer membrane, two other unknown mechanisms are indicated with question-marks: the export of yersinopine to the extracellular space and the import of a yersinopine-metal complex to the periplasm.

Materials and Methods

Bacterial strains, plasmids and culture conditions

The strains used in this study and their characteristics are listed in Supplementary Table 2. All the strains were grown aerobically with horizontal shaking at 28°C in the minimum medium TMH supplemented or not with various concentrations of EDTA (as necessary). 5.10^6 cells per milliliter of culture were inoculated from overnight cultures into 50 mL of media in round clear polystyrene sterile bottles of 250 mL (Easy Grip Corning, VWR). To avoid any metal contamination, all the media were prepared using plastic materials and sterilized by filtration (0.22 µm pore size). Growth was monitored by measuring the optical density at 600 nm over time.

Mutant construction

E. coli DH5α-pir was used to replicate suicide plasmids. *Y. pseudotuberculosis* labelled mutants were constructed via allelic exchange with DNA fragments cloned into suicide plasmid pDS132 (see Supplementary Table 2). Recombinant plasmids were introduced into *Y. pseudotuberculosis* via conjugation with the *E. coli* S17.1-λpir donor (35). *Y. pestis* labelled mutants were constructed by Red recombination using pEP1436 as previously described (36, 37). In mutants of both species, antibiotic resistance genes were eventually deleted via the FLP activity encoded by pFLP3. The pFLP3 plasmid was then cured on sucrose 5%.

The *Y. pseudotuberculosis* and *Y. pestis cnt::lacZ* reporter strains were constructed by selecting chromosomal integration of suicide plasmids pEP696 or pEP620 on kanamycin. These plasmids were introduced by conjugation with the *E. coli* S17.1-λpir donor (35).

We used the ExocET procedure (38) to clone the *Y. pseudotuberculosis cntPQRLMI* operon as a 6.8-kb XbaI-BglII insert and generate pEP699. To complement *Y. pseudotuberculosis* Δ*cntQ*(RLMI), the XbaI-BglII fragment from pEP699 was cloned into pEP1046 opened with SpeI and BamHI to generate pEP701 bearing miniTn7T-Zeo2-*cntPQRLMI*. Triparental mating of the recipient *Y. pseudotuberculosis* strain with *E. coli* S17.1λpir(pEP701) and S17.1λpir(pTNS3) followed by selection on zeocin allowed for the recombinant miniTn7 transfer. Correct chromosomal integration was checked by PCR.

Growth curves and generation time

Overnight cultures were grown aerobically with horizontal shaking at 28°C in TMH medium using polycarbonate Erlenmeyer flasks. From these overnight cultures, three independent biological replicates were inoculated at OD (600 nm) of 0.05 in fresh TMH medium supplemented with various concentrations of EDTA (from 0 to 800 µM) in clear, flat bottom, 96-well plates (Corning™ Costar 3596). Growths were recorded in a Tecan Spark Microplate Incubator/Reader (Thermo Fisher Scientific) for 24 hours at 28°C under continuous shaking and with 600 nm absorbance measurements every 15 min. All measures were corrected with the absorbance of non-inoculated media. Growth curves were analyzed with R studio and generation times were estimated by using the GrowthCurver Package (39).

Genome analysis, protein cloning, expression and purification

The web interface MaGe MicroScope was used to evaluate the syntheny of the *cnt* genes and to compare their sequence from different strains of *Y. pestis* and *Y. pseudotuberculosis* (40). The genes encoding the YpCntLM locus (*yptb1372-1373*) were amplified by PCR from genomic DNA of *Y. pseudotuberculosis* IP32777 using specific primers. The primers used in this study are listed in Table 2. Q5® High-Fidelity DNA polymerase (New England BioLabs). Amplified DNA was cloned in pET-SUMO following the standard protocol (ChampionTM pET SUMO Protein Expression System, Invitrogen). This intermediate plasmid was then used as a template to amplify and clone independently the cntL and cntM genes cloned in pET-SUMO. Sequencing was performed after cloning to evaluate the absence of mutation. *Escherichia coli* One ShotTM BL21 (DE3) bearing the pRARE plasmid was then transformed with the recombinant plasmids (pRARE encodes tRNA genes for rare codons in *E. coli*). Bacterial cultures were grown at 37°C in LB media supplemented with kanamycin at 50 $\mu g.ml^{-1}$ and chloramphenicol at 25 $\mu g.ml^{-1}$, with horizontal shaking. When the OD (600 nm) of the culture reached 0.6, protein expression was induced by the addition of 0.1 mM IPTG. After overnight growth in LB at 16°C, cells were recovered by centrifugation at 5 000 g for 20 min at 4°C. Cells were resuspended in buffer A (20 mM Na_2HPO_4, 300mM NaCl, 15 mM imidazole, pH = 7.5) supplemented with DNase and anti-protease. The cells were then disrupted using a French press (Amico) operating at 1 000 psi. Cell debris were removed by centrifugation at 8 000 *g* for 20 min at 4°C. The supernatants were centrifuged at 115 000 *g* for 45 min at 4°C to remove cell wall debris and membrane proteins. The resulting soluble fraction was loaded on a nickel affinity column (HisTrap 1 mL column, G.E. Healthcare), and proteins were eluted stepwise with buffer B (20mM Na2HPO4,

300mM NaCl, 500 mM imidazole, pH = 7.5), with 20% for washing and 100% for elution. Eluted proteins were transferred into imidazole-free buffer B (20mM Na_2HPO_4, 300mM NaCl, 10% glycerol, pH = 7.5). Protein purity was evaluated by performing a gel electrophoresis using NuPage–10%BisTris gels (Invitrogen).

Detection of yersinopine by TLC assay

TLC assay had been used to detect staphylopine, pseudopaline and bacillopaline in previous studies (7, 8, 28, 41). This experiment consists in incubating purified enzymes with various substrates including one labeled with ^{14}C to follow the reaction and the production of the metabolite of interest. In this study, the YpCntL and YpCntM proteins (2.5 µM) were mixed with carboxyl-[^{14}C]-labeled SAM (2.5 µM), L- or D-histidine (1 mM), NADPH or NADH (10 µM) and pyruvate or α-ketoglutarate (1 mM). The total volume of the reactions was 100 µL in a buffer composed of 50 mM of HEPES, 1 mM of DTT and 1 mM of EDTA (pH=9). The mixtures were incubated for 30 min at 28°C. Reactions were stopped by adding ethanol to a final concentration of 50% (v/v) and the products were separated by thin-layer chromatography (TLC). An aliquot of 10 µL of each reaction mixture was spotted on HPTLC (High-Performance TLC) Silica Gel 60 Glass Plates (Merck KGaA). The HPTLC plates were developed with a phenol:n-butanol:formate:water (12:3:2:3, v/v) solvent system, dried and exposed to a [^{14}C]-sensitive imaging plate for one day. Imaging plates were scanned on a Typhoon FLA 7000 phosphorimager (GE Healthcare).

Sample preparation and detection of yersinopine by HILIC/ESI-MS

In vitro incubations and culture supernatants were prepared and analysed by HILIC/ESI-MS to detect the presence of yersinopine. To prepare the *in vitro* samples, the purified enzymes YpCntL and YpCntM were mixed with SAM (2.5 µM), L-histidine (1 mM), NADPH or NADH (10 µM) and pyruvate or α-ketoglutarate (1 mM). After 30 min of incubation at 28°C, the reactions were stopped by freezing and stored at -80°C prior analysis. For the culture supernatants (extracellular fraction), *Y. pestis* and *Y. pseudotuberculosis* were grown in TMH medium during 24 h in aerobic conditions at 28°C. After centrifugation (5 000 g for 20 min at 4°C), the supernatants were collected, filtered (0.22 µm pore size) and stored at -80°C prior analysis. To perform HILIC separations, an Agilent 1100 capillary HPLC system (Agilent, Tokyo, Japan) was coupled to an LTQ Orbitrap Velos mass spectrometer (Thermo Fisher Scientific, Bremen,

Germany). The HILIC column used for the separations was a TSK gel amide 80 (250 mm x 1 mm i.d., 5 µm) from Tosoh Biosciences (Stuttgart, Germany). Gradient elution, at a flow rate of 50 $\mu l.min^{-1}$, was carried out using acetonitrile (eluent A), and eluent B, 10 mM ammonium formate (pH 5.5). The gradient program was: 0–2 min: 20% B, 2–17 min: up to 50% B, 17–21 min: 50% B, 21–23 min: up to 65% B, 23–25 min: 65% B, 25–30 min: down to 20% B, 30–35 min: 20% B. Samples were diluted with acetonitrile and water to obtain a 1:2, sample to acetonitrile ratio, and centrifuged. An aliquot of 7 µl of the supernatant was injected into the HILIC column for each analysis. To get accurate masses, MS spectra were recalibrated offline using precursor/fragment ions with known formula.

Analysis of metal concentration by ICP-MS

Y. pestis and *Y. pseudotuberculosis* were grown in TMH medium in aerobic conditions at 28°C. After 24 h of growth, 25 mL of the culture were centrifuged (4 000 g for 20 min at 4°C). The pellets were recovered, washed three times with ammonium acetate (20 mM), and dried at 50°C during 48 h. Metal contents were determined in cell fraction by resuspending the dried pellets with a 200 µL mixture of 70% HNO_3 (100 µL) and 30% H_2O_2 (100 µL). The mixtures were heated at 80°C for 3 h and then diluted with water to reach a final volume of 2 mL. Acidified sample solutions were analyzed by ICP-MS (Agilent 7500cs) operating in hydrogen collision gas mode (H_2) to remove possible interferences.

Statistical analysis

ICP-MS measurements of metal concentrations were performed in 2 or 3 independent biological triplicates, done on 2 or 3 different days (depending on the strains). To analyze all the data together, we normalized the metal content of each strain to the WT for each independent experiment. Statistical analyses were performed on R Studio (version 4.1.1). The metal content of the deletion strains was compared to the wild-type using a Welch test after checking for normality. p-values were adjusted by the Bonferroni method for multiple testing.

Acknowledgements

We thank the Agence Nationale de la Recherche for initial support [grant ANR-14-CE09-0007-02], the french ministry of research for a PhD grant awarded to CL. FS was partly supported by the ERC Synergy project Synergy-Plague (101118880). We would like to thank Pierre Lê-Bury

and Javier Pizarro-Cerda (Institut Pasteur) as well as members of both Arnoux and Sebbane teams for support and discussions. Richard C. Allen and Ikram Hammar are acknowledged respectively for advice on statistical analysis and illustration of the model.

References

1. Chandrangsu P, Rensing C, Helmann JD. 2017. Metal homeostasis and resistance in bacteria. 6. Nat Rev Microbiol 15:338–350.
2. Ma Z, Jacobsen FE, Giedroc DP. 2009. Coordination Chemistry of Bacterial Metal Transport and Sensing. Chemical Reviews 109:4644–4681.
3. Weinberg ED. 1975. Nutritional Immunity: Host's Attempt to Withhold Iron From Microbial Invaders. JAMA 231:39–41.
4. Hood MI, Skaar EP. 2012. Nutritional immunity: transition metals at the pathogen–host interface. Nature Reviews Microbiology 10:525–537.
5. Zygiel EM, Nolan EM. 2018. Transition Metal Sequestration by the Host-Defense Protein Calprotectin. Annual Review of Biochemistry 87:621–643.
6. Nelson CE, Huang W, Zygiel EM, Nolan EM, Kane MA, Oglesby AG. 2021. The Human Innate Immune Protein Calprotectin Elicits a Multimetal Starvation Response in *Pseudomonas aeruginosa*. Microbiology Spectrum 9:e00519-21.
7. Ghssein G, Brutesco C, Ouerdane L, Fojcik C, Izaute A, Wang S, Hajjar C, Lobinski R, Lemaire D, Richaud P, Voulhoux R, Espaillat A, Cava F, Pignol D, Borezee-Durant E, Arnoux P. 2016. Biosynthesis of a broad-spectrum nicotianamine-like metallophore in *Staphylococcus aureus*. Science 352:1105–1109.
8. Lhospice S, Gomez NO, Ouerdane L, Brutesco C, Ghssein G, Hajjar C, Liratni A, Wang S, Richaud P, Bleves S, Ball G, Borezée-Durant E, Lobinski R, Pignol D, Arnoux P, Voulhoux R. 2017. *Pseudomonas aeruginosa* zinc uptake in chelating environment is primarily mediated by the metallophore pseudopaline. Sci Rep 7:17132.
9. Mastropasqua MC, D'Orazio M, Cerasi M, Pacello F, Gismondi A, Canini A, Canuti L, Consalvo A, Ciavardelli D, Chirullo B, Pasquali P, Battistoni A. 2017. Growth of *Pseudomonas aeruginosa* in zinc poor environments is promoted by a nicotianamine-related metallophore. Mol Microbiol 106:543–561.
10. Grim KP, San Francisco B, Radin JN, Brazel EB, Kelliher JL, Párraga Solórzano PK, Kim PC, McDevitt CA, Kehl-Fie TE. 2017. The Metallophore Staphylopine Enables *Staphylococcus aureus* To Compete with the Host for Zinc and Overcome Nutritional Immunity. MBio 8.
11. Laffont C, Arnoux P. 2020. The ancient roots of nicotianamine: diversity, role, regulation and evolution of nicotianamine-like metallophores. Metallomics 12:1480–1493.
12. Hossain S, Morey JR, Neville SL, Ganio K, Radin JN, Norambuena J, Boyd JM, McDevitt CA,

Kehl-Fie TE. 2023. Host subversion of bacterial metallophore usage drives copper intoxication. mBio 14:e0135023.

13. Fojcik C, Arnoux P, Ouerdane L, Aigle M, Alfonsi L, Borezée-Durant E. 2018. Independent and cooperative regulation of staphylopine biosynthesis and trafficking by Fur and Zur. Mol Microbiol 108:159–177.
14. Morey JR, Kehl-Fie TE. 2020. Bioinformatic Mapping of Opine-Like Zincophore Biosynthesis in Bacteria. mSystems 5:e00554-20.
15. McFarlane JS, Davis CL, Lamb AL. 2018. Staphylopine, pseudopaline, and yersinopine dehydrogenases: A structural and kinetic analysis of a new functional class of opine dehydrogenase. J Biol Chem 293:8009–8019.
16. Achtman M, Zurth K, Morelli G, Torrea G, Guiyoule A, Carniel E. 1999. *Yersinia pestis*, the cause of plague, is a recently emerged clone of *Yersinia pseudotuberculosis*. Proceedings of the National Academy of Sciences 96:14043–14048.
17. Hinnebusch BJ, Chouikha I, Sun Y-C. 2016. Ecological Opportunity, Evolution, and the Emergence of Flea-Borne Plague. Infection and Immunity 84:1932–1940.
18. Chain PSG, Carniel E, Larimer FW, Lamerdin J, Stoutland PO, Regala WM, Georgescu AM, Vergez LM, Land ML, Motin VL, Brubaker RR, Fowler J, Hinnebusch J, Marceau M, Medigue C, Simonet M, Chenal-Francisque V, Souza B, Dacheux D, Elliott JM, Derbise A, Hauser LJ, Garcia E. 2004. Insights into the evolution of *Yersinia pestis* through whole-genome comparison with *Yersinia pseudotuberculosis*. Proc Natl Acad Sci U S A 101:13826–13831.
19. Sebbane F, Devalckenaere A, Foulon J, Carniel E, Simonet M. 2001. Silencing and reactivation of urease in *Yersinia pestis* is determined by one G residue at a specific position in the ureD gene. Infect Immun 69:170–176.
20. Chouikha I, Hinnebusch BJ. 2014. Silencing urease: a key evolutionary step that facilitated the adaptation of *Yersinia pestis* to the flea-borne transmission route. Proc Natl Acad Sci U S A 111:18709–18714.
21. Remy L, Carrière M, Derré-Bobillot A, Martini C, Sanguinetti M, Borezée-Durant E. 2013. The *Staphylococcus aureus* Opp1 ABC transporter imports nickel and cobalt in zinc-depleted conditions and contributes to virulence. Molecular Microbiology 87:730–743.
22. Perry RD, Bobrov AG, Fetherston JD. 2015. The Role of Transition Metal Transporters for Iron, Zinc, Manganese, and Copper in the Pathogenesis of *Yersinia pestis*. Metallomics 7:965–978.

23. Forman S, Paulley JT, Fetherston JD, Cheng Y-Q, Perry RD. 2010. Yersinia ironomics: comparison of iron transporters among *Yersinia pestis* biotypes and its nearest neighbor, *Yersinia pseudotuberculosis*. Biometals 23:275–294.
24. Desrosiers DC, Bearden SW, Mier I, Abney J, Paulley JT, Fetherston JD, Salazar JC, Radolf JD, Perry RD. 2010. Znu Is the Predominant Zinc Importer in *Yersinia pestis* during In Vitro Growth but Is Not Essential for Virulence. Infect Immun 78:5163–5177.
25. Bobrov AG, Kirillina O, Fetherston JD, Miller MC, Burlison JA, Perry RD. 2014. The *Yersinia pestis* siderophore, yersiniabactin, and the ZnuABC system both contribute to zinc acquisition and the development of lethal septicaemic plague in mice. Mol Microbiol 93:759–775.
26. Behnsen J, Zhi H, Aron AT, Subramanian V, Santus W, Lee MH, Gerner RR, Petras D, Liu JZ, Green KD, Price SL, Camacho J, Hillman H, Tjokrosurjo J, Montaldo NP, Hoover EM, Treacy-Abarca S, Gilston BA, Skaar EP, Chazin WJ, Garneau-Tsodikova S, Lawrenz MB, Perry RD, Nuccio S-P, Dorrestein PC, Raffatellu M. 2021. Siderophore-mediated zinc acquisition enhances enterobacterial colonization of the inflamed gut. 1. Nat Commun 12:7016.
27. Price SL, Vadyvaloo V, DeMarco JK, Brady A, Gray PA, Kehl-Fie TE, Garneau-Tsodikova S, Perry RD, Lawrenz MB. 2021. Yersiniabactin contributes to overcoming zinc restriction during *Yersinia pestis* infection of mammalian and insect hosts. Proceedings of the National Academy of Sciences 118:e2104073118.
28. Laffont C, Brutesco C, Hajjar C, Cullia G, Fanelli R, Ouerdane L, Cavelier F, Arnoux P. 2019. Simple rules govern the diversity of bacterial nicotianamine-like metallophores. Biochem J 476:2221–2233.
29. Li Y, Qiu Y, Gao H, Guo Z, Han Y, Song Y, Du Z, Wang X, Zhou D, Yang R. 2009. Characterization of Zur-dependent genes and direct Zur targets in *Yersinia pestis*. BMC Microbiology 9:128.
30. Gu Y, Liu Y, Mao W, Peng Y, Han X, Jin H, Xu J, Chang L, Hou Y, Shen X, Liu X, Yang Y. 2024. Functional versatility of Zur in metal homeostasis, motility, biofilm formation, and stress resistance in *Yersinia pseudotuberculosis*. Microbiology Spectrum 12:e03756-23.
31. Wang T, Yang X, Gao F, Zhao C, Kang Y, Wang Y, Shen X. 2016. Zinc acquisition via ZnuABC in *Yersinia pseudotuberculosis* facilitates resistance to oxidative stress. 3. Ann Microbiol 66:1189–1197.
32. Lerat E, Ochman H. 2005. Recognizing the pseudogenes in bacterial genomes. Nucleic

Acids Res 33:3125–3132.

33. Forman S, Nagiec MJ, Abney J, Perry RD, Fetherston JD. 2007. Analysis of the aerobactin and ferric hydroxamate uptake systems of *Yersinia pestis*. Microbiology (Reading) 153:2332–2341.
34. Pederick VG, Eijkelkamp BA, Begg SL, Ween MP, McAllister LJ, Paton JC, McDevitt CA. 2015. ZnuA and zinc homeostasis in *Pseudomonas aeruginosa*. Scientific Reports 5:13139.
35. Simon R, Priefer U, Pühler A. 1983. A Broad Host Range Mobilization System for In Vivo Genetic Engineering: Transposon Mutagenesis in Gram Negative Bacteria. Nat Biotechnol 1:784–791.
36. Pradel E, Lemaître N, Merchez M, Ricard I, Reboul A, Dewitte A, Sebbane F. 2014. New Insights into How Yersinia pestis Adapts to Its Mammalian Host during Bubonic Plague. PLoS Pathogens 10:e1004029.
37. Dewitte A, Bouvenot T, Pierre F, Ricard I, Pradel E, Barois N, Hujeux A, Bontemps-Gallo S, Sebbane F. 2020. A refined model of how Yersinia pestis produces a transmissible infection in its flea vector. PLOS Pathogens 16:e1008440.
38. Wang H, Li Z, Jia R, Yin J, Li A, Xia L, Yin Y, Müller R, Fu J, Stewart AF, Zhang Y. 2018. ExoCET: exonuclease in vitro assembly combined with RecET recombination for highly efficient direct DNA cloning from complex genomes. Nucleic Acids Res 46:e28.
39. Sprouffske K, Wagner A. 2016. Growthcurver: an R package for obtaining interpretable metrics from microbial growth curves. BMC Bioinformatics 17:172.
40. Vallenet D, Calteau A, Dubois M, Amours P, Bazin A, Beuvin M, Burlot L, Bussell X, Fouteau S, Gautreau G, Lajus A, Langlois J, Planel R, Roche D, Rollin J, Rouy Z, Sabatet V, Médigue C. 2020. MicroScope: an integrated platform for the annotation and exploration of microbial gene functions through genomic, pangenomic and metabolic comparative analysis. Nucleic Acids Research 48:D579–D589.
41. Higuchi K, Suzuki K, Nakanishi H, Yamaguchi H, Nishizawa NK, Mori S. 1999. Cloning of nicotianamine synthase genes, novel genes involved in the biosynthesis of phytosiderophores. Plant Physiology 119:471–480.
42. Rose RE. 1988. The nucleotide sequence of pACYC177. Nucleic Acids Research 16:356.
43. Philippe N, Alcaraz J-P, Coursange E, Geiselmann J, Schneider D. 2004. Improvement of pCVD442, a suicide plasmid for gene allele exchange in bacteria. Plasmid 51:246–255.
44. Choi K-H, Gaynor JB, White KG, Lopez C, Bosio CM, Karkhoff-Schweizer RR, Schweizer HP.

2005. A Tn7-based broad-range bacterial cloning and expression system. Nat Methods 2:443–448.

45. Datsenko KA, Wanner BL. 2000. One-step inactivation of chromosomal genes in *Escherichia coli* K-12 using PCR products. Proceedings of the National Academy of Sciences 97:6640–6645.
46. Bibi-Triki S, Li de la Sierra-Gallay I, Lazar N, Leroy A, Van Tilbeurgh H, Sebbane F, Pradel E. 2014. Functional and Structural Analysis of HicA3-HicB3, a Novel Toxin-Antitoxin System of *Yersinia pestis*. Journal of Bacteriology 196:3712–3723.

Supplementary Figures and Tables:

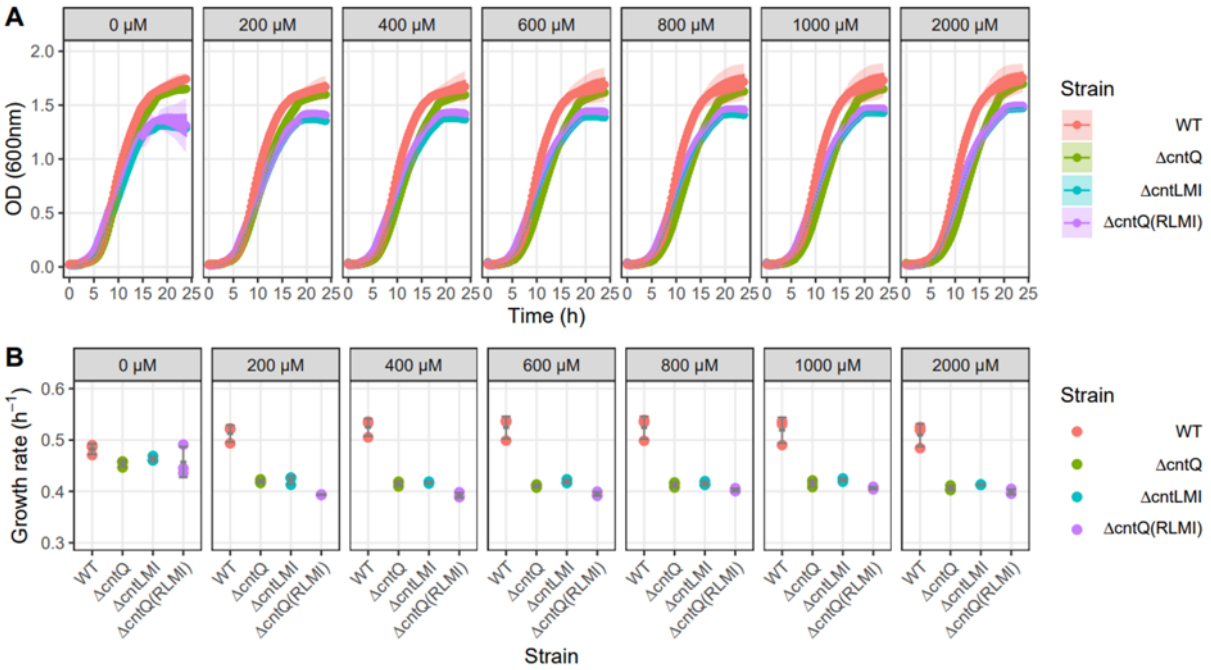

Supplementary Figure 1: Growth curves (A) and inferred growth rates (B) of *Y. pseudotuberculosis* cultivated in TMH without or with increasing concentration of EDTA. In A, the data represent the means and the confidence intervals (95%) calculated from three biological replicates. In B, the data from these three biological replicates are shown as individual points associated with their mean and standard deviation (in grey).

Organism	Label	maxLrap	minLrap	Ident %	Eval	OrderQ	OrderB	BeginQ	EndQ	LengthQ	BeginB	EndB	LengthB
Yersinia pseudotuberculosis IP 32953	YPTB1370	1,00	1,00	100	2,42E-192	1	1	1	352	352	1	352	352
Yersinia pseudotuberculosis PB1/+	YPTS_1469	1,00	1,00	100	2,42E-192	1	1	1	352	352	1	352	352
Yersinia pseudotuberculosis YPIII	YPK_2719	1,00	1,00	99	9,13E-192	1	1	1	352	352	1	352	352
Yersinia pseudotuberculosis IP 31758	YpsIP31758_2634	1,00	1,00	99	3,50E-191	1	1	1	352	352	1	352	352
Yersinia pestis Nepal516	YPN_2640	0,46	0,54	100	1,46E-85	1	1	190	352	352	138	300	300
Yersinia pestis Nepal516	YERNE_2722	0,31	0,86	99	1,33E-54	3	1	79	188	352	1	110	128
Yersinia pestis Nepal516	YERNE_2723	0,20	0,92	97	1,30E-33	8	1	1	72	352	1	72	78
Yersinia pestis CO92	YPO1344	0,46	0,54	100	1,50E-85	1	1	190	352	352	139	301	301
Yersinia pestis CO92	YERPE_1369	0,31	0,86	99	1,37E-54	3	1	79	188	352	1	110	128
Yersinia pestis CO92	YERPE_1368	0,20	0,92	97	1,33E-33	8	1	1	72	352	1	72	78
Yersinia pestis KIM	y2839	0,46	0,58	100	1,49E-85	1	1	190	352	352	118	280	280
Yersinia pestis KIM	y2838	0,32	0,86	99	7,22E-56	3	1	77	188	352	1	112	130
Yersinia pestis KIM	y2840	0,20	0,87	97	1,32E-33	8	1	1	72	352	6	77	83
Yersinia pestis D106004	YPD4_1189	0,45	1,00	100	8,95E-83	1	1	195	352	352	1	158	158
Yersinia pestis D106004	YPD4_1188	0,31	0,86	99	1,35E-54	3	1	79	188	352	1	110	128
Yersinia pestis D106004	YERPDc_1422	0,20	0,92	97	1,31E-33	8	1	1	72	352	1	72	78
Yersinia pestis biovar Orientalis PEXU2	YERP2_13281	0,45	1,00	100	9,22E-83	1	1	195	352	352	1	158	158
Yersinia pestis biovar Orientalis PEXU2	YERP2_13280	0,31	0,86	99	1,39E-54	3	1	79	188	352	1	110	128
Yersinia pestis biovar Orientalis PEXU2	YERP2_13279	0,20	0,92	97	1,35E-33	8	1	1	72	352	1	72	78
Yersinia pestis biovar Mediaevalis K1973002	YERPM_20240	0,40	1,00	100	3,81E-73	1	1	211	352	352	1	142	142
Yersinia pestis biovar Mediaevalis K1973002	YERPM_20241	0,31	0,86	99	1,36E-54	3	1	79	188	352	1	110	128
Yersinia pestis biovar Mediaevalis K1973002	YERPM_20242	0,20	0,92	97	1,32E-33	8	1	1	72	352	1	72	78
Yersinia pestis biovar Orientalis F1991016	YERPF_10236	0,40	1,00	100	3,93E-73	1	1	211	352	352	1	142	142
Yersinia pestis biovar Orientalis F1991016	YERPF_10237	0,31	0,86	99	1,40E-54	3	1	79	188	352	1	110	128
Yersinia pestis biovar Orientalis F1991016	YERPF_10238	0,20	0,92	97	1,37E-33	8	1	1	72	352	1	72	78
Yersinia pestis biovar Orientalis India 195	YERPO_90280	0,45	1,00	100	9,05E-83	1	1	195	352	352	1	158	158
Yersinia pestis biovar Orientalis India 195	YERPO_90279	0,31	0,86	99	1,36E-54	3	1	79	188	352	1	110	128
Yersinia pestis biovar Orientalis India 195	YERPO_90278	0,20	0,92	97	1,33E-33	8	1	1	72	352	1	72	78
Yersinia pestis biovar Antiqua B42003004	YERP4_20352	0,45	1,00	100	9,33E-83	1	1	195	352	352	1	158	158
Yersinia pestis biovar Antiqua B42003004	YERP4_20350	0,20	0,92	97	1,37E-33	8	1	1	72	352	1	72	78
Yersinia pestis biovar Antiqua B42003004	YERP4_20351	0,32	0,86	99	7,45E-56	3	1	77	188	352	1	112	130
Yersinia pestis CA88-4125	YERPCc_20318	0,45	1,00	100	9,02E-83	1	1	195	352	352	1	158	158
Yersinia pestis CA88-4125	YERPCc_20317	0,31	0,86	99	1,36E-54	3	1	79	188	352	1	110	128
Yersinia pestis CA88-4125	YERPCc_20316	0,20	0,92	97	1,32E-33	8	1	1	72	352	1	72	78
Yersinia pestis Pestoides F	YPDSF_2355	0,46	0,54	100	1,45E-85	1	1	190	352	352	138	300	300
Yersinia pestis Pestoides F	YERPN_2489	0,31	0,86	99	1,32E-54	3	1	79	188	352	1	110	128
Yersinia pestis Pestoides F	YERPN_2490	0,20	0,92	97	1,29E-33	8	1	1	72	352	1	72	78
Yersinia pestis D182038	YPD8_0957	0,45	1,00	100	8,87E-83	1	1	195	352	352	1	158	158
Yersinia pestis D182038	YERP1c_1143	0,31	0,86	99	1,34E-54	3	1	79	188	352	1	110	128
Yersinia pestis D182038	YERP1c_1144	0,20	0,92	97	1,30E-33	8	1	1	72	352	1	72	78
Yersinia pestis biovar Antiqua E1979001	YERP9_50170	0,45	1,00	100	9,32E-83	1	1	195	352	352	1	158	158
Yersinia pestis biovar Antiqua E1979001	YERP9_50169	0,31	0,86	99	1,40E-54	3	1	79	188	352	1	110	128
Yersinia pestis biovar Antiqua E1979001	YERP9_50168	0,20	0,92	97	1,36E-33	8	1	1	72	352	1	72	78
Yersinia pestis biovar Microtus str, 91001	YP_1252	0,46	0,58	100	1,49E-85	1	1	190	352	352	118	280	280
Yersinia pestis biovar Microtus str, 91001	YER91_1269	0,31	0,86	99	1,36E-54	3	1	79	188	352	1	110	128
Yersinia pestis biovar Microtus str, 91001	YER91_1270	0,20	0,92	97	1,33E-33	8	1	1	72	352	1	72	78
Yersinia pestis Angola	YpAngola_A1574	0,41	1,00	100	6,57E-75	1	1	208	352	352	1	145	145
Yersinia pestis Angola	YpAngola_A1574	0,32	0,86	99	6,83E-56	3	1	77	188	352	1	112	130
Yersinia pestis Angola	YpAngola_A1574	0,20	0,92	97	1,25E-33	8	1	1	72	352	1	72	78
Yersinia pestis Antiqua	YPA_0630	0,46	0,54	100	1,52E-85	1	1	190	352	352	138	300	300
Yersinia pestis Antiqua	YERPA_0653	0,31	0,86	99	1,38E-54	3	1	79	188	352	1	110	128
Yersinia pestis Antiqua	YERPA_0652	0,20	0,92	97	1,35E-33	8	1	1	72	352	1	72	78
Yersinia pestis Pestoides A	YERPPA_250040	0,30	1,00	100	8,39E-52	3	1	248	352	352	1	105	105
Yersinia pestis Pestoides A	YERPPA_250038	0,31	0,86	99	1,38E-54	2	1	79	188	352	1	110	128
Yersinia pestis Pestoides A	YERPPA_250037	0,20	0,92	97	1,35E-33	8	1	1	72	352	1	72	78
Yersinia pestis biovar Antiqua UG05-0454	YERPU_20097	0,40	1,00	100	3,88E-73	1	1	211	352	352	1	142	142
Yersinia pestis biovar Antiqua UG05-0454	YERPU_20098	0,31	0,86	99	1,39E-54	3	1	79	188	352	1	110	128
Yersinia pestis biovar Antiqua UG05-0454	YERPU_20099	0,20	0,92	97	1,35E-33	8	1	1	72	352	1	72	78

Supplementary Table 1: Pseudogenization of cntQ permease is conserved in Y. pestis strains. List of orfs predicted in sequenced *Y. pseudotuberculosis* and *Y. pestis* strains at the *cntQ* position. maxLrap and minLrap denote respectively the length (expressed as a percentage of the gene) that is conserved, taking YPTB1370 as a reference.

Supplementary Table 2: Bacterial strains and plasmids used in this study

Strain name in the text	*Description*
Yersinia pseudotuberculosis	
Y. pseudotuberculosis WT	*Y. pseudotuberculosis* IP32777
Y. pseudotuberculosis Δ*lacZ cntP*$_P$::*lacZ* (Zur+)	IP32777 Δ*lacZ cntP*$_P$::*lacZ* chromosomal *lacZ* reporter fusion with *cnt* promoter
Y. pseudotuberculosis Δ*lacZ cntP*$_P$::*lacZ* (*Z*ur-)	IP32777 Δ*lacZ* Δ*zur cntP*$_P$::*lacZ* *zur* deletion and *lacZ* reporter fusion with *cnt* promoter
Y. pseudotuberculosis ΔcntLMI	IP32777 Δ*cntLMI*-FRT unlabeled deletion of *cntLMI*
Y. pseudotuberculosis ΔcntQ(RLMI)	IP32777 Δ*cntQ*::Km1447 *cntQ* deletion and insertion of a kanamycin resistance cassette abolishing *cntRLMI* expression
Y. pseudotuberculosis ΔcntQ	IP32777 Δ*cntQ*-FRT derived from YPEP153, unlabeled deletion of *cntQ,* no polar effect on *cntRLMI* downstream genes
Y. pseudotuberculosis ΔcntQ(RLMI) complemented	IP32777 Δ*cntQ*::Km1447 mini-Tn7-Zeo2::*cntPQRLMI* Strain complemented by the insertion of *cntPQRLMI*
Yersinia pestis	
Y. pestis WT	*Y. pestis* KIM6+

Y. pestis ΔcntLMI	KIM6+ Δ*cntLMI*::Tp1087 *cntLMI* deletion and insertion of a trimethoprim (Tp) resistance cassette
Y. pestis ΔcntQ(RLMI)	KIM6+ Δ*cntQ*::Km1447 *cntQ* deletion and insertion of a kanamycin resistance cassette cassette abolishing *cntRLMI* expression
Y. pestis Δ*lacZ cntP*$_P$::*lacZ* (Zur+)	KIM6+ Δ*lacZ cntP*$_P$::*lacZ* chromosomal *lacZ* reporter fusion with *cnt* promoter
Y. pestis Δ*lacZ cntP*$_P$::*lacZ* (Zur-)	KIM6+ Δ*lacZ* Δ*zur cntP*$_P$::*lacZ* *zur* deletion and *lacZ* reporter fusion with *cnt* promoter
Y. pestis ΔcntQ(RLMI) ΔybtX	KIM6+ Δ*cntQ*::Km1447 Δ*ybtX*::TpNP *ybtX* deletion and insertion of a Tp resistance cassette without polar effect on downstream *ybt* genes
Y. pestis ΔcntLMI ΔznuCB	KIM6+ Δ*cntLMI*::Tp1087 Δ*znuCB*::Km4 Deletion of *znuCB* and insertion of a kanamycin resistance cassette
Y. pestis ΔcntQ(RLMI) ΔybtX ΔznuCB	KIM6+ Δ*cntQ*::Km1447 Δ*ybtX*::TpNP Δ*znuCB*::Sm1315 Deletion of *znuCB* and inserting a streptomycin resistance cassette
Plasmids	

Name	Description	Reference
pACYC177	Suicide plasmid used as a template to generate pEP699 by ExoCET cloning.	(42)
pDS132	Suicide plasmid, CmR.	(43)
pFLP3	Encodes FLP recombinase to excise FRT flanked cassettes.	(44)
pKD4	Source of Km R cassette, Km flanked by FRT sites.	(45)
pEP620	lacZ reporter suicide plasmid bearing Pcnt from *Y. pestis.*	
pEP681	pDS132:: DcntQ::Km1447, CmR KmR	
pEP692	pDS132::DcntLMI::Tp1087, CmR TpR	
pEP696	lacZ reporter suicide plasmid bearing Pcnt from *Y. pseudotuberculosis*, derived from pEP848.	
pEP699	p15A-Ap::cntPQRLMI, obtained by ExoCET cloning of the *Y. pseudotuberculosis cnt* operon.	
pEP701	pUC18R6K-miniTn7-Zeo2-cntPQRLMI, *cnt* operon from *Y. pseudotuberculosis.*	
pEP848	lacZ reporter suicide plasmid, KmR.	EP, personal collection
pEP1046	Delivery plasmid for mini-Tn7T-Zeo2.	GenBank MH614591
pEP1087	Source of TpR cassette flanked by FRT sites.	(46)

pEP1315	Source of SmR cassette flanked by FRT sites.	GenBank MH626523
pEP1436	Plasmid used for Red recombination in *Y. pestis*.	(37)
pEP1447	Source of Km1447 cassette flanked by FRT sites, in this plasmid the Km resistance gene is oriented opposite to that in pEP1436.	(37)